Estuarine, Coastal and Shelf Science 250 (2021) 107113

Contents lists available at ScienceDirect

Estuarine, Coastal and Shelf Science

journal homepage: http://www.elsevier.com/locate/ecss

Ocean acidification increases phytobenthic carbon fixation and export in a warm-temperate system

Shigeki Wada [a,*], Sylvain Agostini [a], Ben P. Harvey [a], Yuko Omori [b], Jason M. Hall-Spencer [a,c]

[a] Shimoda Marine Research Center, University of Tsukuba, Shimoda, Japan
[b] Life and Environmental Sciences, University of Tsukuba, Tsukuba, Japan
[c] School of Biological and Marine Sciences, University of Plymouth, Plymouth, UK

ARTICLE INFO

Keywords:
Carbon cycle
CO_2 seep
Diatoms
Macroalgae
Marine productivity

ABSTRACT

The response of photosynthetic organisms to rising CO_2 levels is a key topic in ocean acidification research. Most of the work in this field has focused on physiological responses in laboratory conditions which lack ecological realism. Studies using seeps as natural analogues for ocean acidification have demonstrated shifts in algal community composition, but the effect of CO_2 on carbon fixation and export remains unclear. Here, we deployed artificial substrata in a warm-temperate region of Japan to collect algal communities using a CO_2 seep off Shikine Island. Diatoms became dominant on settlement substrata in areas with elevated CO_2 levels, whereas macroalgae dominated at present-day levels of CO_2 (reference site). This was supported by pigment composition; fucoxanthin content, characteristic of diatoms, was higher at the high CO_2 site, while more Chlorophyll *b*, which is characteristic of Chlorophyta, was found in the reference site. Algal communities that recruited in water with high levels of CO_2 had elevated rates of photosynthesis. Algal biomass was similar on all settlement panels, regardless of CO_2 concentration. Much of the carbon that was fixed by algae in the high CO_2 conditions was exported, likely due to detachment from the substratum. Diatoms that dominated under high CO_2 conditions are more easily transported away as they have no holdfast, whereas newly settled macroalgae became firmly attached at present-day levels of CO_2. These results show that ocean acidification may fundamentally alter coastal carbon cycling, increasing photosynthesis and carbon export from coastal ecosystems in warm-temperate biogeographic regions due to a shift in community composition from perennial to ephemeral algae.

1. Introduction

Benthic algae are the major primary producers in shallow coastal regions (Charpy-Roubaud and Sournia, 1990), and they have a number of other important ecological roles such as a source of energy, carbon storage and habitat provisioning (Smale et al., 2013; Costanza et al., 2014). Recent work has shown that rising carbon dioxide levels influence these functions (Hall-Spencer and Harvey, 2019). Uptake of anthropogenic CO_2 is causing surface ocean seawater pH to fall by around 0.002 units per year with a 100% increase in the concentration of H^+ ions projected for the end of this century (IPCC, 2013). Ocean acidification is a serious threat to coastal ecosystems because it reduces the saturation state of carbonate which can make seawater corrosive to calcifying organisms such as hard corals and shellfish (Doney et al., 2020).

As well as reducing the availability of calcium carbonate, ocean acidification increases the amount of dissolved inorganic carbon (DIC) and this can stimulate the growth of certain photosynthetic organisms (Hendriks et al., 2010; Olischläger and Wiencke, 2013), if sufficient nutrients are available (Celis-Plá et al., 2015). Many algae benefit from increased seawater CO_2 concentrations in laboratory tests (Gao et al., 1991; Kubler et al., 1999; Liu et al., 2018) although the response is species-specific because some algae have carbon concentrating mechanisms (CCM) adapted to present day low CO_2 conditions (Badger et al., 1998; Cornwall et al., 2017).

To assess changes to coastal carbon cycling, we need to consider both the physiological responses of algae to ocean acidification, and the changes in community composition. In areas where CO_2 is released from volcanic seeps the gas dissolves into seawater providing a natural analogue for the effects of ocean acidification (Hall-Spencer et al., 2008) which include profound changes to benthic microalgal (Johnson et al., 2013) and macroalgal communities at both individual and population

* Corresponding author. Shimoda Marine Research Center, University of Tsukuba, Shimoda, 415-0025, Japan.
E-mail address: swadasbm@shimoda.tsukuba.ac.jp (S. Wada).

https://doi.org/10.1016/j.ecss.2020.107113
Received 26 May 2020; Received in revised form 6 November 2020; Accepted 15 November 2020
Available online 3 December 2020

levels (Porzio et al., 2011, 2018, 2020). At a recently characterised natural analogue site in Japan, calcifying algae and large habitat-forming macroalgae get replaced by turf algae at elevated CO_2 levels (Agostini et al., 2015, 2018; Harvey et al., 2019). This has been observed at many other shallow-water CO_2 seeps worldwide, although at some seeps seagrasses grow well (Hall-Spencer et al., 2008; Connell et al., 2018). In the present study, we assess how a CO_2 gradient at a Japanese seep affects algal community composition, photosynthesis and biomass production.

Measurements of photosynthesis at CO_2 seeps allow us to better constrain projections of the response of primary producers to ocean acidification. In addition, comparison of photosynthesis and biomass production furthers our understanding of carbon storage by coastal ecosystems. Previous studies taking this approach have assessed specific algal taxa (Hofmann et al., 2015; Vogel et al., 2015; Connell et al., 2018), but the effects of ocean acidification on benthic algal community photosynthesis had not previously been investigated. To tackle this, we used settlement panels which are widely used to easily collect natural benthic communities (Perkol-Finkel et al., 2006; Sokołowski et al., 2017). This technique has been used to assess shifts in benthic community composition along CO_2 gradients in the Mediterranean (Lidbury et al., 2012; Johnson et al., 2013; Kroeker et al., 2013b). Moreover, settlement panels also allow the investigation of the abundance, diversity and production of those communities of organisms that recruit on to them.

In the present study, we investigated high CO_2 and present-day conditions off Shikine Island, Japan. After 44 and 72 days we collected algal communities that had recruited *in situ*, recorded differences in community composition, incubated them in light conditions to measure net photosynthesis, and then analysed the photosynthetic pigments present. Our aim was to assess how high CO_2 conditions affect coastal carbon fixation and storage.

2. Materials and methods

2.1. Study sites

We deployed algal settlement panels in and away from a CO_2 seep that is well characterised as an analogue for ocean acidification (Agostini et al., 2015, 2018). It is located off Mikawa Bay, Shikine Island (139.2°N, 34.3°E) in Japan (Fig. 1). Two sites were used, an acidified area near to the CO_2 seep (the 'high CO_2 site') and a nearby area (the 'reference site') in an adjacent bay of the island. The high CO_2 site provided an end-of-the-century projection for reductions in pH (IPCC, 2013), and was not confounded by differences in temperature, salinity, dissolved oxygen, total alkalinity, nutrients or depth relative to the reference site (Agostini et al., 2015, 2018; Harvey et al., 2019). Agostini et al. (2018) and Harvey et al. (2018) present the environmental and carbonate chemistry data collected during the present study. Briefly, seawater pH in total scale (pH_T) and other environmental parameters were monitored using a combination of sensors (interval of measurement was 15 or 30 min, recorded from 25th May to July 5th' 2016) and discrete water sampling for total alkalinity. For reference and high CO_2 sites, pH_T was 8.137 ± 0.056 and 7.809 ± 0.093 respectively, the salinity was 34.5 ± 0.43 and 34.1 ± 0.69, the temperature was 19.7 ± 0.71 and 19.5 ± 0.82 °C, the total alkalinity was 2270 ± 15.4 and 2270 ± 20.3 μmol kg^{-1} and the calculated pCO_2 levels were 309 ± 46.4 and 769 ± 225 μatm (mean ± SD).

2.2. Deployment of settlement panels

Settlement panels were held at −5 m depth Chart Datum within the high CO_2 and reference sites. The panels were made of transparent PVC measuring 5 × 2 × 0.2 cm. A total of 76 panels were attached to floats anchored 1 m above the seafloor and haphazardly spread over a surface of ca. 400 m^2 in each site. In April 2016, we put four and five floats in the high CO_2 and reference sites, respectively, corresponding to 34 panels in the high CO_2 and 42 panels in the reference sites. Subsets of the panels were retrieved in June after 44 days and July (after 72 days). The algae on the panels were examined using a light microscope.

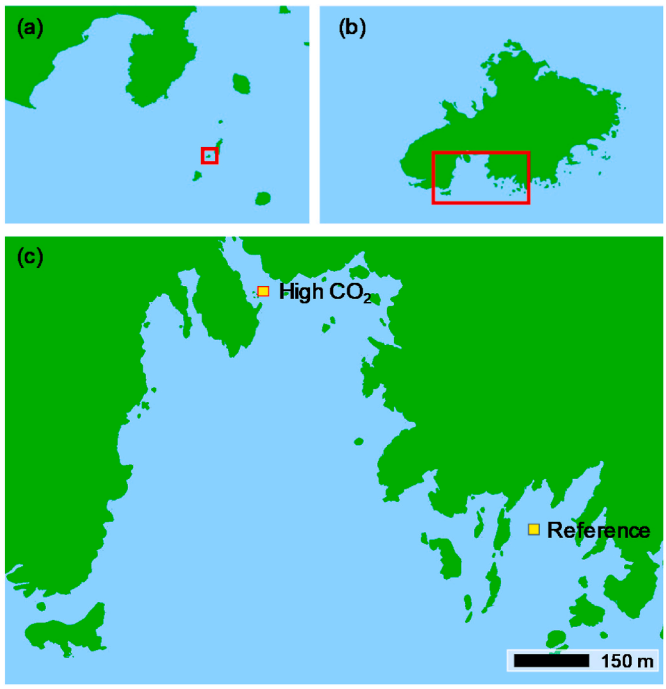

Fig. 1. Study area off the Izu peninsula and archipelago off mainland Japan (a), Shikine Island (b) and the locations for the reference and high CO2 site used for the deployment of settlement panels (c), land shown in green. (For interpretation of the references to colour in this figure legend, the reader is referred to the Web version of this article.)

2.3. Pigment analysis

After 44 and 72 days of deployment, 19 and 5 panels from the high CO_2, and 18 and 12 panels from the reference site were retrieved (at random) for pigment analysis. Each settlement panel was photographed and analysed with imaging software (Adobe, Photoshop) to measure the area size of the panels, and then stored at −80 °C for pigment analysis. The surface of each panel was scraped clean and the settled organisms were put into 8 ml N'N-dimethylformamide to extract photosynthetic pigments. Canthaxanthin was added to the extracts as an internal standard, and this was then filtered through a polytetrafluorethylene (PTFE) filter with pore size of 0.45 μm (GE Healthcare Life Science, Whatman™ syringe filter, 13 mm diameter). Aliquot of extracts was injected into an isocratic high-performance liquid chromatograph (Agilent, 1100 system controlled by ChemStation) equipped with a C8 column (Agilent, Zorbax Eclipse XDB-C8; 4.6 × 150 mm, 3.5 μm) and diode-array and fluorescent detectors. The peak of each pigment was identified by comparison of their retention time relative to eight standards; fucoxanthin, prasinoxanthin, 19′-hexanoloxyfucoxanthin, diadinoxanthin, alloxanthin, zeaxanthin, Chlorophyll *b* and Chlorophyll *a* (Chl *a*), as described in more detail in Hama et al. (2016).

2.4. Net photosynthesis

After 44 and 72 days of deployment, 6 and 4 panels from the high CO_2, and 6 and 6 panels from the reference site were retrieved (at random) for the measurement of net photosynthesis (NP). Incubation was carried out using a 250 ml acid-cleaned polycarbonate bottle, with a subset of each panel (0.8 × 2.5 cm) being used. Each bottle was filled

with seawater collected from the site where the panels were retrieved, and incubated under light (150 μmol photon s^{-1} cm^{-2}) at 20 °C for 1 h to measure rates of NP. Dissolved oxygen (DO) concentrations and pH in NBS scale (pH_{NBS}) were measured at the start and end of the incubation period with an optode DO meter (WTW, FD0925) and a multi-sensor (ThermoFisher Scientific, Orion StarTM, equipped with a ROSS pH electrode, 8156BNUWP). Based on the change in DO concentrations (ΔDO) values, we calculated the NP rates (normalised by unit area) using the following equations:

NP_{area} (NP per unit area: μg O_2 cm^{-2} hour $^{-1}$) = ΔDO × $V/A/T$ × 1000.where V, A and T are volume of seawater for incubation (l), area of the plate (cm^2), and incubation time (hour), respectively (Roth et al., 2019).

Following the incubation, each settlement panel was photographed and analysed with imaging software (Adobe, Photoshop) to measure the exact panel area size. All incubations were completed within 6 h of collecting the panels.

2.5. Statistical analysis

The amount of Chl *a* and the rates of NP_{area} were analysed using a two-way linear mixed model (LMM) (R package: nlme, function: lme; *v3.1-147*: Pinheiro et al., 2020) with 'Site' and 'Days' as fixed factors. Since several panels were attached to each float, 'float' was treated as a random factor. Homogeneity of variance (Levene Test) and normality (QQ plot) were assessed for Chl *a* and NP_{area}. Both Chl *a* (following log transformation) and NP_{area} conformed to these assumptions. Weighted principal component analysis (R package: aroma light, functions: wpca: Bengtsson et al., 2010), followed by PERMANOVA (R package: vegan, function: adonis; *v2.5-6*: Oksanen et al., 2019), were used to assess for differences in the composition of accessory pigments between 'Site' and 'Days'. Weighting for the principal component analysis was used to improve the robustness to uneven group sample sizes, with weighting applied to each sample individually as 1/n, where n is the sample size of the respective treatment groups (combinations of 'Site' and 'Days'). In the present study, all statistical analyses were performed using the R statistical software, version 3.5.1 (R Core Team, 2018), and visualisations were produced using ggplot 2 (Wickham, 2016) and ggpubr (Kassambara, 2020).

3. Results

Visual inspection of the panels revealed biofilm formation and algal recruitment on all panels across both sites and time points. At the high CO_2 site, the panel were covered with a homogenous brown biofilm at both time points (Fig. 2a and b). Panels at the reference site were covered with a more diverse range of algal recruits (Fig. 2c and d). After 72 days, the panels were more overgrown relative to 44 days, with juvenile macroalgal Chlorophyta dominating panels at the reference site whereas the diatoms *Triceratium* sp. and *Biddulphia* sp. were dominant on settlement panels at the high CO_2 site (Fig. 2e–g).

Chl *a* was the main pigment and accounted for 31–68% of the total weight of pigments per sample. The amount of Chl *a* per unit area of the plates deployed in the high CO_2 and reference sites was 0.284 ± 0.048 μg cm^{-2} and 0.285 ± 0.022 and on day 44, and increased to 1.86 ± 0.27 μg cm^{-2} and 2.03 ± 0.13 and on day 72, respectively (Fig. 3). While Chl *a* value significantly increased from day 44–72 (LMM, 'Days': $F_{1,5}$ = 93.49, p < 0.001), there was no significant difference between the two sites (LMM, 'Site' x 'Days', $F_{1,5}$ = 4.68, p = 0.083) (Table S1). Fucoxanthin was the second most abundant pigment, and the ratios of Fuc/Chl *a* on the panels from high CO_2 site were 1.01 ± 0.082 (n = 18) and 0.488 ± 0.041 (n = 5) on day 44 and 72, respectively. These values were relatively higher than those from reference site (0.724 ± 0.036 (n = 16) and 0.485 ± 0.070 (n = 12) on day 44 and 72, respectively).

The overall composition of the pigments differed between both the 'Site' (PERMANOVA: $F_{1,\ 47}$ = 27.44, p < 0.001) and 'Days' (PERMANOVA: $F_{1,\ 47}$ = 13.22, p < 0.001), but did not show a significant interaction (PERMANOVA: $F_{1,\ 47}$ = 1.92, p = 0.16) (Table S2). Principal component analysis showed that the two sites (high CO_2 and reference) were mostly separated along PC1 (accounting for 28.8% of total variance; Fig. S1) with values in a negative and positive direction distinguishing the high CO_2 and reference sites, respectively (Fig. 4). The pigment fucoxanthin showed a loading of −0.55 on the PC1 and therefore had a moderate contribution towards explaining the high CO_2 site (Table 1). Chl *b* showed a positive loading of 0.70 and therefore had a moderate contribution towards explaining the reference site (Table 1). The proportion of fucoxanthin among accessory pigments were generally higher at the high CO_2 site compared to the reference site, whereas the proportion of chlorophyll *b* was higher in the reference site, and below detection limit at day 44 in the High CO_2 site (Table 1). The two 'Days' (44 and 72) were mostly separated along PC2 (accounting for 20.1% of total variance; Fig. S1) with values in a negative and positive direction distinguishing the earlier (day 44) and latter (day 72) sampling points, respectively (Fig. 4). Prasinoxanthin, diadinoxanthin, and 19′-hexanoloxyfucoxanthin had a moderate contribution (−0.70, −0.53 and −0.31, respectively) towards explaining the earlier and latter sampling points (Table 1). Of these pigments, diadinoxanthin represented between 9 and 19% of the total accessories pigments, although the other

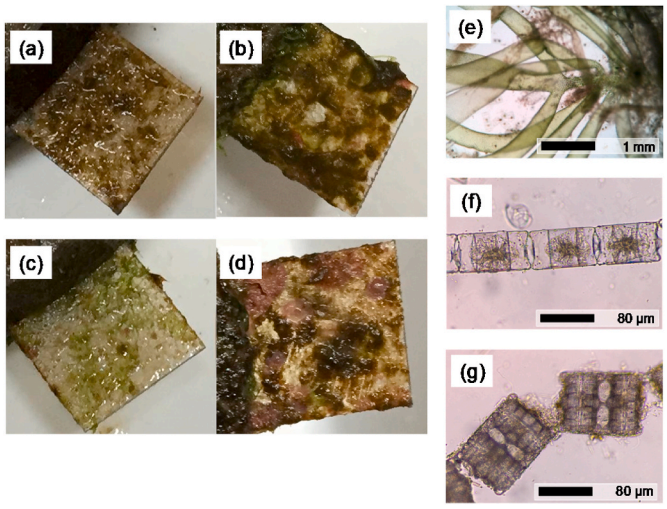

Fig. 2. Panels retrieved from high CO2 (a and b on day 44 and 72) and reference sites (c and d on day 44 and 72). Macroalgae dominated on settlement panels at the reference site (e), diatoms dominated at the acidified site; Triceratium sp. (f) and Biddulphia sp. (g).

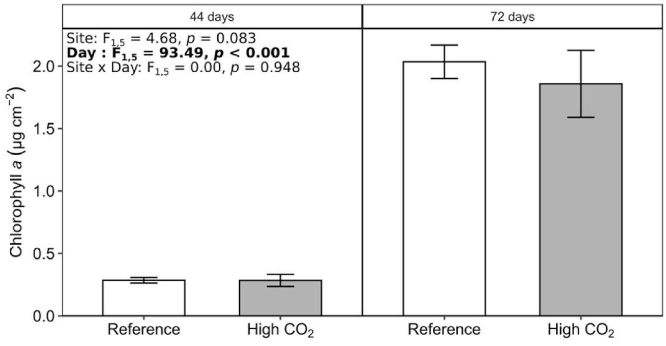

Fig. 3. Mean Chlorophyll *a* per unit area of the panels (μg cm-2) of panels at Reference (white) and High CO2 (grey) sites after 44 and 72 days. Error bars show standard error (n = 18, 18, 12, 5). The statistical significance (linear mixed model on log-transformed data) of the main effects (Day and Site) and their interaction is shown.

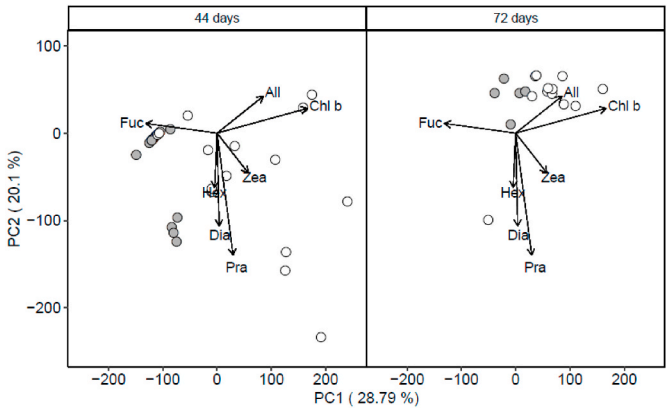

Fig. 4. Weighted principal component analysis biplot of accessory pigments across site (High CO2, filled circles, Reference - empty circles) and time points (44 days - left, and 72 days - right). The same PCA is used for both panels, but time points were separated for ease of visualisation, with the loading of each pigment indicated by vectors. The accessory pigments are fucoxanthin (Fuc), prasinoxanthin (Pra), 19′-hexanoloxyfucoxanthin (Hex), diadinoxanthin (Dia), alloxanthin (All), zeaxanthin (Zea) and chlorophyll *b* (Chl b).

two pigments (Prasinoxanthin and 19′- hexanoloxyfucoxanthin) represented less than 5% (Table 1). The two other pigments, Alloxanthin and Zeaxanthin were minor components, contributing less than 4.2% each to the total accessory pigments (Table 1).

The pH_{NBS} values of the seawater collected from the high CO_2 and\ reference sites (at 20 °C) were 7.92 ± 0.003 and 8.20 ± 0.006 on day 44, and 7.70 ± 0.009 and 8.16 ± 0.007 (mean ± SD) on day 72, respectively. The changes in pH_{NBS} (ΔpH_{NBS}) under light incubation for the sample from high CO_2 and reference sites were 0.068 ± 0.007 and 0.043 ± 0.008 on day 44, and 0.046 ± 0.020 and 0.052 ± 0.006 (mean ± SD) on day 72, respectively, reflecting CO_2 consumption by photosynthesis. Since the changes in the pH_{NBS} during the incubations were within narrow ranges (from 0.023 to 0.081), differences in pH_{NBS} between the seawater collected from the high CO_2 and reference sites were maintained throughout the experiment. The concentrations of DO at the start of light incubations were 8.73–9.48 mg l^{-1}, and changes in the incubation period were 0.18–0.93 mg l^{-1}.

Net photosynthesis rates (NP_{area}) of the panels from the high CO_2 site were 16.5 ± 1.3 (mean ± SE, n = 6) and 31.7 ± 1.8 (mean ± SE, n = 4) μg O_2 cm^{-2} $hour^{-1}$ on day 44 and 72, and from the reference site were 6.94 ± 0.71, (mean ± SE, n = 6) and 21.8 ± 2.6, (mean ± SE, n = 6) μg O_2 cm^{-2} $hour^{-1}$ on day 44 and 72, respectively (Fig. 4). Overall, this meant that NP_{area} of the settlement panels was significantly greater on Day 72 compared to Day 44 (LMM: 'Day', $F_{1,5} = 34.29$, $p < 0.01$), and also higher at the high CO_2 site relative to the reference site (LMM: 'Site', $F_{1,5} = 10.41$, $p < 0.05$) (Fig. 5, Table S3).

4. Discussion

Studies of carbon dioxide seeps worldwide have shown that increasing levels of ocean acidification cause major shifts in coastal algal community composition (Hall-Spencer and Harvey, 2019). Here we show that algal settlement is affected by increasing levels of CO_2. Macroalgal recruits dominated settlement panels at a reference site, being well attached by holdfasts, whereas less firmly attached diatoms dominated on panels at a high CO_2 site (Fig. 2). The differences in algal communities were confirmed through photosynthetic pigment analysis. The amount of fucoxanthins was higher in the algal communities at high CO_2, these pigments are common in heterokont algae such as diatoms and brown algae (Dring, 1998; Kuczynska et al., 2015).

Microscopy showed that diatoms, rather than brown algae, dominated the early stages of settlement at high CO_2, and this was confirmed by our pigment analyses after 44 and 72 days of settlement on panels. The pigment composition of brown algae and benthic diatom mats reported in previous studies show that the ratio of Fuc/Chl *a* in most brown algae (mean values among 30 species: 0.372; Colombo-Pallotta et al., 2006; Desmond et al., 2019; Marambio et al., 2017; Seely et al., 1972; Verma et al., 2017; Méndez et al., 2019) were lower than those of natural diatom mats (mean values among 4 reports: 1.168; Sundback et al., 1996; Wulff et al., 2005, 2008; Stief et al., 2013) (Table S4).

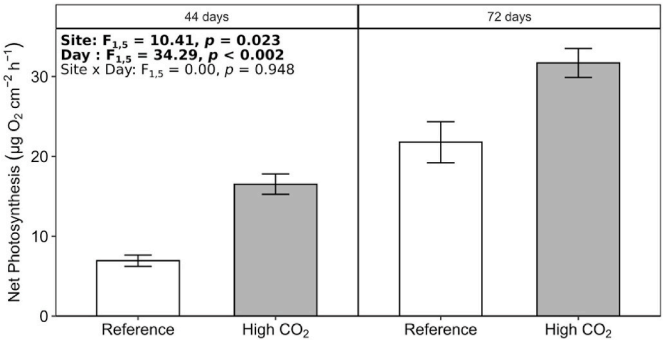

Fig. 5. Net photosynthetic rates during laboratory incubation of panels from Reference (white bars) and High CO2 (grey bars) sites and time points (44 and 72 days) in seawater sampled at the same site. Error bars show standard error (n = 6, 6, 6, 4, respectively). The statistical significance (linear mixed model) of the main effects (Day and Site) and their interaction is shown.

Table 1
PCA loadings of the different pigments (across both sites and time points), and their percentage weights (mean ± se (n)) for each site and time point.

			Percentage Weight			
	PCA loading		44 days after		72 days after	
Pigment	PC1	PC2	Reference	High CO_2	Reference	High CO_2
Alloxanthin	0.36	0.21	1.8 ± 0.5 (16)	0.2 ± 0.2 (18)	1.2 ± 0.2 (12)	2.1 ± 0.1 (5)
Chlorophyll *b*	0.70	0.14	7.1 ± 2 (16)	0 ± 0 (18)	7.8 ± 1.1 (12)	2.9 ± 1.2 (5)
Diadinoxanthin	0.02	−0.53	12.4 ± 0.3 (16)	14.9 ± 0.3 (18)	11.7 ± 0.4 (12)	12.4 ± 0.6 (5)
Fucoxanthin	−0.55	0.06	72.8 ± 2.4 (16)	84 ± 0.4 (18)	72.9 ± 1 (12)	79.3 ± 1.4 (5)
19′-Hexanoloxyfucoxanthin	0.02	−0.31	0.8 ± 0.6 (16)	0 ± 0 (18)	5 ± 0.6 (12)	3.1 ± 0.3 (5)
Prasinoxanthin	0.12	−0.70	0.9 ± 0.5 (16)	0.9 ± 0.4 (18)	0.3 ± 0.3 (12)	0 ± 0 (5)
Zeaxanthin	0.24	−0.23	4.2 ± 0.7 (16)	0 ± 0 (18)	1.1 ± 0.3 (12)	0.2 ± 0.2 (5)

Considering the higher ratio of Fuc/Chl *a* on the panels from the high CO_2 site, this confirms that benthic diatoms were dominant at the high CO_2 site. In contrast, there was significantly more Chl *b* in the algal community that settled onto the Reference site panels (Table 1), and this is the main accessory pigment of Chlorophyta (Dring, 1998). Studies worldwide show that benthic diatoms seem to be capable of benefitting from ocean acidification/high CO_2 conditions (Johnson et al., 2013; Marques da Silva et al., 2017; Harvey et al., 2019). Deployment of settlement panels at this site showed that diatom recruitment was more intense in the high CO_2 site than in reference conditions.

Our study sites off Shikine island were very exposed to wave action and are in the path of a strong ocean current (Kuroshio current), so it is worth comparing our results with those from experiments set up in more sheltered conditions. Recruitment of algae using artificial substrata have been assessed at CO_2 seeps off the islands of Vulcano and Ischia in Italy which are both less exposed to strong water movement than Shikine Island. Off Vulcano, Johnson et al. (2013) also found higher diatom abundance at high CO_2 on settlement substrata suspended in the water column, but did not report on export of the biomass grown in these conditions. Off Ischia island CO_2 seeps, volcanic stone tiles were attached to the seafloor to monitor algal succession for 2–14 months (Kroeker et al., 2012; Porzio et al., 2013). Contrary to the present study, only a minimal biomass of diatoms was reported at high CO_2. As the panels in the present study were suspended off the seafloor, benthic herbivores, such as gastropods, did not have access to the floats to graze. Since grazing pressure is an important driving force in the community composition of benthic flora (Hillebrand et al., 2000), the deployment position of the artificial substrata (suspended or attached) could lead to differences in successional processes. In addition to the environmental condition and experimental set-up, the duration of the experimental deployment represents another important factor determining algal community succession. Our experiment examined the phase of early succession, so there is scope in future studies to investigate the effects of ocean acidification on the long-term development of biofouling communities as it takes many months for these communities to mature (Kroeker et al., 2013b; Brown et al., 2018).

Net photosynthetic rates were significantly higher on the high CO_2 panels than on the Reference panels (Fig. 5, Table S3), showing an increase in carbon fixation under ocean acidification. In the present day, CO_2 concentrations in surface seawater are generally less than 15 μmol kg^{-1} (Zeebe and Wolf-Gladrow, 2009) which can limit photosynthetic rates, through substrate limitation (Badger et al., 1998). Previous laboratory and aquarium-based studies have shown that increased CO_2 can enhance photosynthesis in some algae (Gao et al., 1991; Kubler et al., 1999; Liu et al., 2018). However, a number of recent studies have found that increased CO_2 can have no or even negative effects on photosynthesis in several algal species (Peach et al., 2017; Porzio et al., 2020), highlighting that responses to ocean acidification are species-specific. These interspecific differences lead to shifts in community composition under high CO_2 conditions, which complicates the up-scaling of laboratory studies to ecosystem-level change. In the present study, we demonstrate that *in situ* photosynthesis of an algal community increased with ocean acidification, which is directly relevant for future projections of primary production and carbon storage.

Although algal community productivity was enhanced in high-CO_2 conditions, the Chl *a* content on these settlement panels was similar to those in reference site conditions (Fig. 3) showing that algal biomass did not increase despite enhanced photosynthesis. This mismatch between photosynthesis and biomass suggests that a large part of the fixed carbon was subsequently being lost in the high-CO_2 conditions due to the detachment of algae and export of carbon from the substratum. In the reference site, macroalgae were held in place by holdfasts which strongly attached the thalli to hard surfaces and helped them resist drag forces due to waves and currents. Diatoms, which were dominant on the panels in the high CO_2 site, have no holdfast and are only attached by sticky mucus materials exuded extracellularly (Hoagland et al., 1993). At our seep site, benthic diatoms were so abundant that they formed turf-like mats in areas with high CO_2 (Fig. S2a and Agostini et al., 2018; Harvey et al., 2019). Detached aggregations of these turf diatoms at the high CO_2 site occur during the spring-summer season, where they can be seen drifting in clumps across the seabed (Figs. S2b and c). The drifting algal aggregates are typically a mixture of diatom and drift macroalgae, with the diatom species identified on the panels (*Triceratium* sp. and *Biddulphia* sp.) found in large numbers within the aggregates (Figs. S2d and e).

Our findings support other research showing that ocean acidification changes coastal algal communities, and we provide novel data showing its effects on coastal carbon fixation and export. Although algae will continue to provide a huge amount of energy for coastal ecosystems through high rates of photosynthesis (Mann, 1973; Graham et al., 2016), our data show a shift from resilient, long-lived, diverse algal stands that store large amounts of carbon, to less resilient, short-lived and less diverse stands that have increased rates of carbon fixation but greater rates of carbon export. Such changes in algal communities reduce habitat complexity and algal biomass in rocky shore habitats. Unless humanity is able to minimize and address the impacts of ocean acidification we can expect that it will cause major disruption to coastal ecosystems with knock-on effects on nearshore food webs, fisheries and carbon cycle.

Declaration of competing interest

The authors declare that they have no known competing financial interests or personal relationships that could have appeared to influence the work reported in this paper.

Acknowledgements

We thank the technical staff of Shimoda Marine Research Center and Mr Yasutaka Tsuchiya, for help with field sampling. We are also grateful to Dr T. Hama for his kind advice. The species identification of diatoms was supported by Drs K. Ishida and T. Nakayama. Dr J. Hama helped with HPLC analysis. The field survey was permitted by Nii-jima Fishery Cooperatives Shikine-jima Branch. This study was supported by the Environment Research and Technology Development Fund (4RF-1701), the Ministry of Education, Science, Sports and Culture, Grant-in-Aid for Scientific Research (B) (19H04234) and Graind-in-Aid for Young Scientists (B) (17K17622), and the International Educational and Research Laboratory Program of the University of Tsukuba.

Appendix A. Supplementary data

Supplementary data to this article can be found online at https://doi.org/10.1016/j.ecss.2020.107113.

Author statement

Shigeki Wada: Conceptualization, Methodology, Investigation, Writing – original draft, Sylvain Agostini: Methodology, Formal analysis, Writing – original draft, Visualisation, Ben P. Harvey: Methodology, Formal analysis, Writing – original draft, Visualisation, Yuko Omori: Investigation, Writing – review & editing, Jason Hall-Spencer: Methodology, Writing – review & editing

References

Agostini, S., Harvey, B.P., Wada, S., Kon, K., Milazzo, M., Inaba, K., Hall-Spencer, J.M., 2018. Ocean acidification drives community shifts towards simplified non-calcified habitats in a subtropical–temperate transition zone. Sci. Rep. 8 https://doi.org/10.1038/s41598-018-29251-7.

Agostini, S., Wada, S., Kon, K., Omori, A., Kohtsuka, H., Fujimura, H., Tsuchiya, Y., Sato, T., Shinagawa, H., Yamada, Y., Inaba, K., 2015. Geochemistry of two shallow CO_2 seeps in Shikine Island (Japan) and their potential for ocean acidification

research. Reg. Stud. Marine Sci. 2, 45–53. https://doi.org/10.1016/j.rsma.2015.07.004.
Badger, M.R., Andrews, T.J., Whitney, S.M., Ludwig, M., Yellowlees, D.C., Leggat, W., Price, G.D., 1998. The diversity and coevolution of Rubisco, plastids, pyrenoids, and chloroplast-based CO_2 -concentrating mechanisms in algae. Can. J. Bot. 76, 1052–1071. https://doi.org/10.1139/b98-074.
Bengtsson, H., Neuvial, P., Speed, T.P., 2010. TumorBoost: normalization of allele-specific tumor copy numbers from a single pair of tumor-normal genotyping microarrays. BMC Bioinf. 11, 245. https://doi.org/10.1186/1471-2105-11-245.
Brown, N.E.M., Milazzo, M., Rastrick, S.P.S., Hall-Spencer, J.M., Therriault, T.W., Harley, C.D.G., 2018. Natural acidification changes the timing and rate of succession, alters community structure, and increases homogeneity in marine biofouling communities. Global Change Biol. 24, e112–e127. https://doi.org/10.1111/gcb.13856.
Celis-Plá, P.S.M., Hall-Spencer, J.M., Horta, P.A., Milazzo, M., Korbee, N., Cornwall, C.E., Figueroa, F.L., 2015. Macroalgal responses to ocean acidification depend on nutrient and light levels. Front. Marine Sci. 2 https://doi.org/10.3389/fmars.2015.00026.
Charpy-Roubaud, C., Sournia, A., 1990. The comparative estimation of phytoplanktonic, microphytobenthic and macrophytobenthic primary production in the oceans'. Mar. Microb. Food Webs 4, 31–57.
Colombo-Pallotta, M.F., García-Mendoza, E., Ladah, L.B., 2006. Photosynthetic performance, light absorption, and pigment composition of *Macrocystis pyrifera* (Laminariales, Phaeophyceae) blades from different depths. J. Phycol. 42, 1225–1234. https://doi.org/10.1111/j.1529-8817.2006.00287.x.
Connell, S.D., Doubleday, Z.A., Foster, N.R., Hamlyn, S.B., Harley, C.D.G., Helmuth, B., Kelaher, B.P., Nagelkerken, I., Rodgers, K.L., Sarà, G., Russell, B.D., 2018. The duality of ocean acidification as a resource and a stressor. Ecology 99, 1005–1010. https://doi.org/10.1002/ecy.2209.
Cornwall, C.E., Revill, A.T., Hall-Spencer, J.M., Milazzo, M., Raven, J.A., Hurd, C.L., 2017. Inorganic carbon physiology underpins macroalgal responses to elevated CO_2. Sci. Rep. 7 https://doi.org/10.1038/srep46297.
Costanza, R., de Groot, R., Sutton, P., van der Ploeg, S., Anderson, S.J., Kubiszewski, I., Farber, S., Turner, R.K., 2014. Changes in the global value of ecosystem services. Global Environ. Change 26, 152–158. https://doi.org/10.1016/j.gloenvcha.2014.04.002.
Desmond, M.J., Pajusalu, L., Pritchard, D.W., Stephens, T.A., Hepburn, C.D., 2019. Whole community estimates of macroalgal pigment concentration within two southern New Zealand kelp forests. J. Phycol. 55, 936–947. https://doi.org/10.1111/jpy.12884.
Doney, S.C., Busch, D.S., Cooley, S.R., Kroeker, K.J., 2020. The impacts of ocean acidification on marine ecosystems and reliant human communities. Annu. Rev. Environ. Resour. 45, 83–112. https://doi.org/10.1146/annurev-environ-012320-083019.
Dring, M.J., 1998. The Biology of Marine Plants. Univ. Press, Cambridge.
Gao, K., Aruga, Y., Asada, K., Ishihara, T., Akano, T., Kiyohara, M., 1991. Enhanced growth of the red alga Porphyra yezoensis Ueda in high CO_2 concentrations. J. Appl. Phycol. 3, 355–362.
Graham, M., Fox, M., Hamilton, S., 2016. Macrophyte productivity and the provisioning of energy and habitat to nearshore systems. In: Ólafsson, E. (Ed.), Marine Macrophytes as Foundation Species. CRC Press, Taylor & Francis Group, 6000 Broken Sound Parkway NW, Suite 300, Boca Raton, FL, pp. 133–152. https://doi.org/10.4324/9781315370781-7, 33487-2742.
Hall-Spencer, J.M., Harvey, B.P., 2019. Ocean acidification impacts on coastal ecosystem services due to habitat degradation. Emerg. Top. Life Sci. 3, 197–206. https://doi.org/10.1042/ETLS20180117.
Hall-Spencer, J.M., Rodolfo-Metalpa, R., Martin, S., Ransome, E., Fine, M., Turner, S.M., Rowley, S.J., Tedesco, D., Buia, M.-C., 2008. Volcanic carbon dioxide vents show ecosystem effects of ocean acidification. Nature 454, 96–99. https://doi.org/10.1038/nature07051.
Hama, T., Inoue, T., Suzuki, R., Kashiwazaki, H., Wada, S., Sasano, D., Kosugi, N., Ishii, M., 2016. Response of a phytoplankton community to nutrient addition under different CO_2 and pH conditions. J. Oceanogr. 72, 207–223. https://doi.org/10.1007/s10872-015-0322-4.
Harvey, B.P., Agostini, S., Kon, K., Wada, S., Hall-Spencer, J.M., 2019. Diatoms dominate and alter marine food-webs when CO_2 rises. Diversity 11, 242. https://doi.org/10.3390/d11120242.
Harvey, B.P., Agostini, S., Wada, S., Inaba, K., Hall-Spencer, J.M., 2018. Dissolution: the achilles' heel of the triton shell in an acidifying ocean. Front. Marine Sci. 5 https://doi.org/10.3389/fmars.2018.00371.
Hendriks, I.E., Duarte, C.M., Álvarez, M., 2010. Vulnerability of marine biodiversity to ocean acidification: a meta-analysis. Estuarine. Coast Shelf Sci. 86, 157–164. https://doi.org/10.1016/j.ecss.2009.11.022.
Hoagland, K.D., Rosowski, J.R., Gretz, M.R., Roemer, S.C., 1993. Diatom extracellular polymeric substances: function, fine structure, chemistry, and physiology. J. Phycol. 29, 537–566. https://doi.org/10.1111/j.0022-3646.1993.00537.x.
Hofmann, L.C., Fink, A., Bischof, K., de Beer, D., 2015. Microsensor studies on *Padina* from a natural CO_2 seep: implications of morphology on acclimation to low pH. J. Phycol. 51, 1106–1115. https://doi.org/10.1111/jpy.12347.
IPCC, 2013. Climate Change 2013: the Physical Science Basis. Contribution of Working Group I to the Fifth Assessment Report of the Intergovernmental Panel on Climate Change. URL. https://www.ipcc.ch/report/ar5/wg1/. accessed 1.10.19.
Johnson, V.R., Brownlee, C., Rickaby, R.E.M., Graziano, M., Milazzo, M., Hall-Spencer, J. M., 2013. Responses of marine benthic microalgae to elevated CO_2. Mar. Biol. 160, 1813–1824. https://doi.org/10.1007/s00227-011-1840-2.
Kassambara, A., 2020. Ggpubr: "Ggplot2" Based Publication Ready Plots.
Kroeker, K.J., Micheli, F., Gambi, M.C., 2013b. Ocean acidification causes ecosystem shifts via altered competitive interactions. Nat. Clim. Change 3, 156–159. https://doi.org/10.1038/nclimate1680.
Kubler, J.E., Johnston, A.M., Raven, J.A., 1999. The effects of reduced and elevated CO_2 and O_2 on the seaweed *Lomentaria articulata*. Plant Cell Environ. 22, 1303–1310. https://doi.org/10.1046/j.1365-3040.1999.00492.x.
Kuczynska, P., Jemiola-Rzeminska, M., Strzalka, K., 2015. Photosynthetic pigments in diatoms. Mar. Drugs 13, 5847–5881. https://doi.org/10.3390/md13095847.
Lidbury, I., Johnson, V., Hall-Spencer, J.M., Munn, C.B., Cunliffe, M., 2012. Community-level response of coastal microbial biofilms to ocean acidification in a natural carbon dioxide vent ecosystem. Mar. Pollut. Bull. 64, 1063–1066. https://doi.org/10.1016/j.marpolbul.2012.02.011.
Liu, L., Zou, D., Jiang, H., Chen, B., Zeng, X., 2018. Effects of increased CO_2 and temperature on the growth and photosynthesis in the marine macroalga Gracilaria lemaneiformis from the coastal waters of South China. J. Appl. Phycol. 30, 1271–1280. https://doi.org/10.1007/s10811-017-1316-y.
Mann, K.H., 1973. Seaweeds: their Productivity and Strategy for Growth: the role of large marine algae in coastal productivity is far more important than has been suspected. Science 182, 975–981. https://doi.org/10.1126/science.182.4116.975.
Marambio, J., Rodriguez, J.P., Mendez, F., Ocaranza, P., Rosenfeld, S., Ojeda, J., Rautenberger, R., Bischof, K., Terrados, J., Mansilla, A., 2017. Photosynthetic performance and pigment composition of Macrocystis pyrifera (Laminariales, Phaeophyceae) along a gradient of depth and seasonality in the ecoregion of Magellan, Chile. J. Appl. Phycol. 29, 2575–2585. https://doi.org/10.1007/s10811-017-1136-0.
Marques da Silva, J., Cruz, S., Cartaxana, P., 2017. Inorganic carbon availability in benthic diatom communities: photosynthesis and migration. Phil. Trans. Biol. Sci. 372, 20160398. https://doi.org/10.1098/rstb.2016.0398.
Méndez, F., Marambio, J., Ojeda, J., Rosenfeld, S., Rodríguez, J.P., Tala, F., Mansilla, A., 2019. Variation of the photosynthetic activity and pigment composition in two morphotypes of Durvillaea Antarctica (Phaeophyceae) in the sub-Antarctic ecoregion of Magallanes, Chile. J. Appl. Phycol. 31, 905–913. https://doi.org/10.1007/s10811-018-1675-z.
Oksanen, J., Blanchet, F.G., Friendly, M., Kindt, R., Legendre, P., McGlinn, D., Minchin, P.R., O'Hara, R.B., Simpson, G.L., Solymos, P., Stevens, M.H.H., Szoecs, E., Wagner, H., 2019. Vegan: community ecology package.
Olischläger, M., Wiencke, C., 2013. Ocean acidification alleviates low-temperature effects on growth and photosynthesis of the red alga Neosiphonia harveyi (Rhodophyta). J. Exp. Bot. 64, 5587–5597. https://doi.org/10.1093/jxb/ert329.
Perkol-Finkel, S., Zilman, G., Sella, I., Miloh, T., Benayahu, Y., 2006. Floating and fixed artificial habitats: effects of substratum motion on benthic communities in a coral reef environment. Mar. Ecol. Prog. Ser. 317, 9–20. https://doi.org/10.3354/meps317009.
Pinheiro, J., Bates, D., DebRoy, S., Sarkar, D., Eispack, E., Heisterkamp, S., Willigen, B.V., R-core, 2020. Nlme: Linear and Nonlinear Mixed Effects Models.
Porzio, L., Arena, C., Lorenti, M., De Maio, A., Buia, M.C., 2020. Long-term response of Dictyota dichotoma var. intricata (C. Agardh) Greville (Phaeophyceae) to ocean acidification: insights from high pCO2 vents. Sci. Total Environ. 731, 138896. https://doi.org/10.1016/j.scitotenv.2020.138896.
Porzio, L., Buia, M.C., Ferretti, V., Lorenti, M., Rossi, M., Trifuoggi, M., Vergara, A., Arena, C., 2018. Photosynthesis and mineralogy of Jania rubens at low pH/high pCO2: a future perspective. Sci. Total Environ. 628, 375–383. https://doi.org/10.1016/j.scitotenv.2018.02.065. –629.
Porzio, L., Buia, M.C., Hall-Spencer, J.M., 2011. Effects of ocean acidification on macroalgal communities. J. Exp. Mar. Biol. Ecol. 400, 278–287. https://doi.org/10.1016/j.jembe.2011.02.011.
R Core Team, 2018. R: A Language and Environment for Statistical Computing. R Foundation for Statistical Computing, Vienna, Austria.
Roth, F., Wild, C., Carvalho, S., Rädecker, N., Voolstra, C.R., Kürten, B., Anlauf, H., El-Khaled, Y.C., Carolan, R., Jones, B.H., 2019. An in situ approach for measuring biogeochemical fluxes in structurally complex benthic communities. Methods Ecol. Evol. 10, 712–725. https://doi.org/10.1111/2041-210X.13151.
Seely, G.R., Duncan, M.J., Vidaver, W.E., 1972. Preparative and analytical extraction of pigments from brown algae with dimethyl sulfoxide. Mar. Biol. 12, 184–188. https://doi.org/10.1007/BF00350754.
Smale, D.A., Burrows, M.T., Moore, P., O'Connor, N., Hawkins, S.J., 2013. Threats and knowledge gaps for ecosystem services provided by kelp forests: a northeast Atlantic perspective. Ecol. Evol. 3, 4016–4038. https://doi.org/10.1002/ece3.774.
Sokołowski, A., Ziółkowska, M., Balazy, P., Kukliński, P., Plichta, I., 2017. Seasonal and multi-annual patterns of colonisation and growth of sessile benthic fauna on artificial substrates in the brackish low-diversity system of the Baltic Sea. Hydrobiologia 790, 183–200. https://doi.org/10.1007/s10750-016-3043-9.
Verma, P., Kumar, M., Mishra, G., Sahoo, D., 2017. Multivariate analysis of fatty acid and biochemical constitutes of seaweeds to characterize their potential as bioresource for biofuel and fine chemicals. Bioresour. Technol. 226, 132–144. https://doi.org/10.1016/j.biortech.2016.11.044.
Vogel, N., Fabricius, K.E., Strahl, J., Noonan, S.H.C., Wild, C., Uthicke, S., 2015. Calcareous green alga *Halimeda* tolerates ocean acidification conditions at tropical carbon dioxide seeps: *halimeda* growing at CO_2 seeps. Limnol. Oceanogr. 60, 263–275. https://doi.org/10.1002/lno.10021.
Wickham, H., 2016. ggplot2: Elegant Graphics for Data Analysis. Springer-Verlag, New York.
Zeebe, R.E., Wolf-Gladrow, D., 2009. CO_2 in Seawater: Equilibrium, Kinetics, Isotopes, vol. 65. Elsevier Oceanography Series.